

## A fast algorithm for 3D azimuthally anisotropic velocity scan

Jingwei Hu<sup>1\*,†</sup>, Sergey Fomel<sup>2</sup> and Lexing Ying<sup>3</sup>

<sup>1</sup>Institute for Computational Engineering and Sciences and Bureau of Economic Geology, The University of Texas at Austin, Austin, TX 78712 USA, <sup>2</sup>Bureau of Economic Geology and Department of Geological Sciences, Jackson School of Geosciences, The University of Texas at Austin TX 78713 USA, and <sup>3</sup>Department of Mathematics and Institute for Computational and Mathematical Engineering, Stanford University, Stanford, CA 94305 USA

Received November 2013, revision accepted June 2014

### ABSTRACT

The conventional velocity scan can be computationally expensive for large-scale seismic data sets, particularly when the presence of anisotropy requires multiparameter scanning. We introduce a fast algorithm for 3D azimuthally anisotropic velocity scan by generalizing the previously proposed 2D butterfly algorithm for hyperbolic Radon transforms. To compute semblance in a two-parameter residual moveout domain, the numerical complexity of our algorithm is roughly  $O(N^3 \log N)$  as opposed to  $O(N^5)$  of the straightforward velocity scan, with  $N$  being the representative of the number of points in a particular dimension of either data space or parameter space. Synthetic and field data examples demonstrate the superior efficiency of the proposed algorithm.

**Key words:** 3D, Velocity analysis, Anisotropic parameter.

### INTRODUCTION

Multiazimuth seismic data reveal the Earth's seismic response along different azimuthal directions. Detecting and measuring the anisotropy in such data can be useful for characterizing fractures or stress in the subsurface (Tsvankin and Grechka, 2011). When apparent azimuthal anisotropy is present, conventional single-parameter isotropic velocity scan and normal moveout (NMO) can be inadequate. To further flatten the events, a residual anisotropic moveout may be necessary. This, however, makes the implementation expensive: the computational cost increases dramatically compared with the single-parameter case. If we assume for simplicity that there are  $N$  sample points in every dimension of the data and model (parameter) domains, then the numerical complexity of a two-parameter velocity scan will be at least  $O(N^5)$ , i.e., summing over  $O(N^2)$  data points for each of  $O(N^3)$  values (time plus two parameters). Furthermore, picking parameters from a high-dimensional semblance volume also poses a

challenge (Adler and Brandwood, 1999; Siliqi *et al.* 2003; Arnaud *et al.* 2004; Tao *et al.* 2012).

In this paper, we introduce a fast algorithm to speed up the velocity-scan process. The stacking procedure involved in computing the semblance can be regarded as a version of the generalized Radon transform (Beylkin, 1984). Following our previous work on 2D hyperbolic Radon transform (Hu *et al.* 2012, 2013), we formulate the time-domain summation as a discrete oscillatory integral in the frequency domain and apply the 3D version of the Fourier integral operator butterfly algorithm (Candès, Demanet, and Ying, 2009). As a result, computational complexity of the velocity scan reduces to roughly  $O(N^3 \log N)$ <sup>1</sup>, where  $N$  is the representative of the number of points in either dimension of data space or model space. An alternative approach to estimating azimuthally anisotropic velocity parameters was developed by Burnett and Fomel (2009a, b) and Casasanta (2011) but may not be applicable to noisy data.

The paper is organized as follows. In the theory part, we first describe an orthogonal anisotropic velocity scan and then give a brief description of the 3D butterfly algorithm and a discussion of its numerical complexity. In the

\*Now at: Department of Mathematics Purdue University, West Lafayette, IN 47907 USA

†E-mail: hu342@purdue.edu

<sup>1</sup> The log function in this paper refers to logarithm to base 2.

second part, we provide two synthetic and one field data examples to test the efficiency and accuracy of the proposed algorithm.

## THEORY

As explained by Grechka and Tsvankin (1998) and Tsvankin and Grechka (2011), a pure-mode (P or S) reflection event in an effectively azimuthally anisotropic medium can be described by

$$t = \sqrt{\tau^2 + W_{11}x^2 + W_{22}y^2 + 2W_{12}xy}, \quad (1)$$

where  $t$  is the two-way common midpoint (CMP) travel time,  $\tau$  is the two-way zero-offset travel time,  $(x, y)$  is the full source–receiver offset in surface survey coordinates, and

$$\mathbf{W} = \begin{pmatrix} W_{11} & W_{12} \\ W_{12} & W_{22} \end{pmatrix} \quad (2)$$

is the slowness squared matrix. Equation (1) follows from a truncated 2D Taylor expansion of  $t^2$ . Geometrically, it represents a curved surface that is hyperbolic in cross section and elliptic in map view.

Ideally, one can perform a semblance scan (Taner and Koehler, 1969) over the three parameters  $W_{11}$ ,  $W_{22}$ , and  $W_{12}$  simultaneously to estimate the slowness matrix and perform NMO correction according to equation (1). However, this approach, if not impossible, is extremely expensive for large-scale seismic data sets. Furthermore, since these parameters are not orthogonal, the semblance plots might appear to be unfocused and ambiguous, hence presenting difficulties for picking (Fowler, Jackson, and Hootman, 2006).

Davidson *et al.* (2011) proposed a stable way of detecting azimuthal anisotropy using orthogonal parameterization of the moveout function, which is based on an equivalent reformulation of equation (1):

$$t = \sqrt{\tau^2 + W_{\text{avg}}(x^2 + y^2) + W_{\text{cos}}(x^2 - y^2) + 2W_{\text{sin}}xy}. \quad (3)$$

The cosine- and sine-dependent slowness values  $W_{\text{cos}}$  and  $W_{\text{sin}}$  are usually much smaller than the averaged slowness  $W_{\text{avg}}$ . Therefore, a possible workflow for anisotropic velocity analysis and NMO correction can proceed in three steps.

- (i) Perform an isotropic velocity scan to estimate  $W_{\text{avg}}$  and flatten seismic events.
- (ii) Perform a residual anisotropic moveout to account for  $W_{\text{cos}}$ - and  $W_{\text{sin}}$ -dependent terms.

- (iii) Convert orthogonal parameters to more intuitive anisotropy parameters. For instance, the NMO velocity at azimuth  $\alpha$  can be recovered by

$$V_{\text{nmo}}^{-2}(\alpha) = W_{\text{avg}} + W_{\text{cos}} \cos 2\alpha + W_{\text{sin}} \sin 2\alpha. \quad (4)$$

In this procedure, the first two steps require a velocity-scan process. Because  $x$  and  $y$  are symmetric in  $W_{\text{avg}}(x^2 + y^2)$ , the single-parameter isotropic scan involved in the first step can be handled efficiently by a 2D butterfly algorithm, as discussed in our previous work (Hu *et al.* 2013). Our goal in this paper is to speed up the more expensive, two-parameter velocity scan in the second step.

To be specific, what we need for residual moveout is to compute a semblance measure (Taner and Koehler, 1969) as follows (assuming that the  $W_{\text{avg}}$  part has been detected in the previous step):

$$S(\tau, W_{\text{cos}}, W_{\text{sin}}) = \frac{\left( \sum_{x,y} d(t(x, y; \tau, W_{\text{cos}}, W_{\text{sin}}), x, y) \right)^2}{N_x N_y \sum_{x,y} d^2(t(x, y; \tau, W_{\text{cos}}, W_{\text{sin}}), x, y)}, \quad (5)$$

where  $d(t, x, y)$  is a 3D CMP data set after isotropic moveout, and

$$t(x, y; \tau, W_{\text{cos}}, W_{\text{sin}}) = \sqrt{\tau^2 + W_{\text{cos}}(x^2 - y^2) + 2W_{\text{sin}}xy}. \quad (6)$$

## Basic formulation

The two summations on the right-hand side of equation (5) are two (discrete) generalized Radon transforms (Beylkin, 1984). Each of them can be expressed generally as (to simplify the notation, we write  $p = W_{\text{cos}}$  and  $q = W_{\text{sin}}$  here and in the following subsections)

$$(Rg)(\tau, p, q) = \sum_{x,y} g(\sqrt{\tau^2 + p(x^2 - y^2) + 2qxy}, x, y), \quad (7)$$

where the function  $g = d$  or  $g = d^2$ .

To construct the fast algorithm, we first rewrite equation (7) in the frequency domain as

$$(Rg)(\tau, p, q) = \sum_{f,x,y} \exp(2\pi i f \sqrt{\tau^2 + p(x^2 - y^2) + 2qxy}) \hat{g}(f, x, y), \quad (8)$$

where  $f$  is the frequency, and  $\hat{g}(f, x, y)$  is the Fourier transform of  $g(t, x, y)$  in time. We next perform a linear transformation to map all discrete points in  $(f, x, y)$  and  $(\tau, p, q)$  domains to points in the unit cube  $[0, 1]^3$ , i.e., a point

**Figure 1** Butterfly tree structure for the special case of  $N = 4$ . The algorithm starts at the top of  $T_X$  and at the bottom of  $T_K$ . It then traverses  $T_X$  top down and  $T_K$  bottom up and terminates at the level  $L = \log N$ . At each level, the computation is done pairwise for every pair of boxes  $(A, B)$ . By construction, their side lengths always satisfy  $w(A)w(B) = 1/N$ ; thus, a low-rank approximation is available.

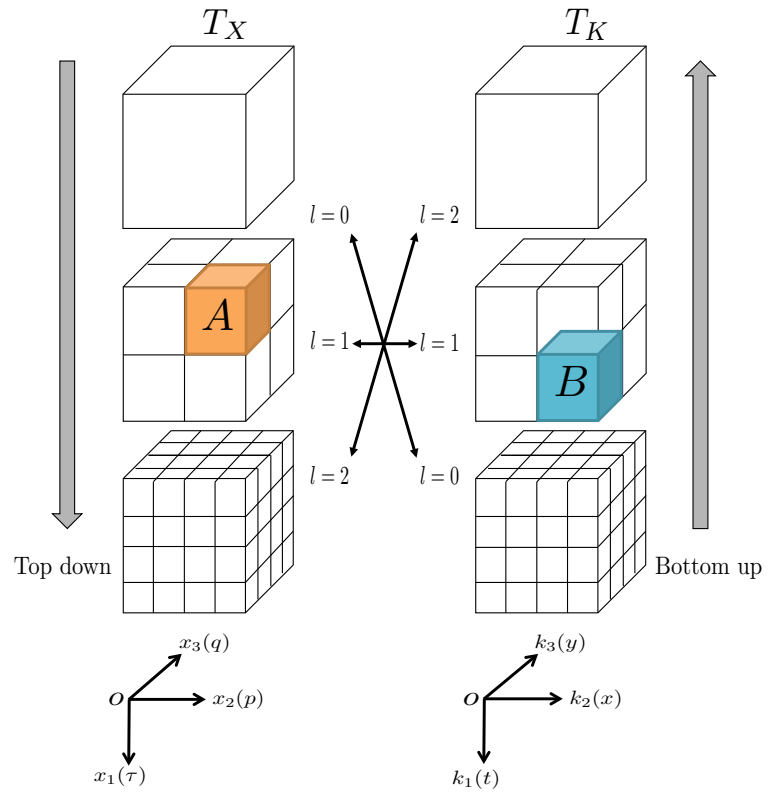


**Table 1** Parameters used to generate the seismic events in Fig. 2(a).

event	$\tau$	$W_{\text{avg}}$	$W_{\text{cos}}$	$W_{\text{sin}}$
1	0.7	0.3	0	0
2	1.8	0.29	0.021	0.021
3	2.6	0.25	-0.01	-0.017
4	3.4	0.15	0	0.02

$(f, x, y) \in [f_{\min}, f_{\max}] \times [x_{\min}, x_{\max}] \times [y_{\min}, y_{\max}]$  is mapped to  $\mathbf{k} = (\mathbf{k}_1, \mathbf{k}_2, \mathbf{k}_3) \in [0, 1] \times [0, 1] \times [0, 1] = K$  via

$$\begin{aligned} f &= (f_{\max} - f_{\min})k_1 + f_{\min}, \\ x &= (x_{\max} - x_{\min})k_2 + x_{\min}, \\ y &= (y_{\max} - y_{\min})k_3 + y_{\min}; \end{aligned}$$

and a point  $(\tau, p, q) \in [\tau_{\min}, \tau_{\max}] \times [p_{\min}, p_{\max}] \times [q_{\min}, q_{\max}]$  is mapped to  $\mathbf{x} = (x_1, x_2, x_3) \in [0, 1] \times [0, 1] \times [0, 1] = X$  via

$$\begin{aligned} \tau &= (\tau_{\max} - \tau_{\min})x_1 + \tau_{\min}, \\ p &= (p_{\max} - p_{\min})x_2 + p_{\min}, \\ q &= (q_{\max} - q_{\min})x_3 + q_{\min}. \end{aligned}$$

If we define a phase function  $\Phi(\mathbf{x}, \mathbf{k})$  as

$$\Phi(\mathbf{x}, \mathbf{k}) = f\sqrt{\tau^2 + p(x^2 - y^2) + 2qxy}, \quad (9)$$

then equation (8) can be recast as

$$(Rg)(\mathbf{x}) = \sum_{\mathbf{k} \in K} \exp(2\pi i \Phi(\mathbf{x}, \mathbf{k})) \hat{g}(\mathbf{k}), \quad \mathbf{x} \in X. \quad (10)$$

### Fast 3D butterfly algorithm

Equation (10) is the discretized form of a 3D oscillatory integral of the type

$$u(\mathbf{x}) = \int_K \exp(2\pi i \Phi(\mathbf{x}, \mathbf{k})) v(\mathbf{k}) d\mathbf{k}, \quad \mathbf{x} \in X, \quad (11)$$

whose fast evaluation can be realized by a butterfly algorithm (Candès, Demanet, and Ying, 2009).

The overall structure of the 3D butterfly algorithm basically follows its 2D analog. The idea is to partition the computational domains  $X$  and  $K$  recursively into a pair of *octrees*<sup>2</sup>,  $T_X$  and  $T_K$ , ending at level  $L = \log N$  (see Fig. 1 for an illustration). Here  $N$  is chosen as an integer power of two, which is on the order of the maximum of  $|\Phi(\mathbf{x}, \mathbf{k})|$  for

<sup>2</sup> An octree is a tree data structure in which each internal node has exactly eight children.

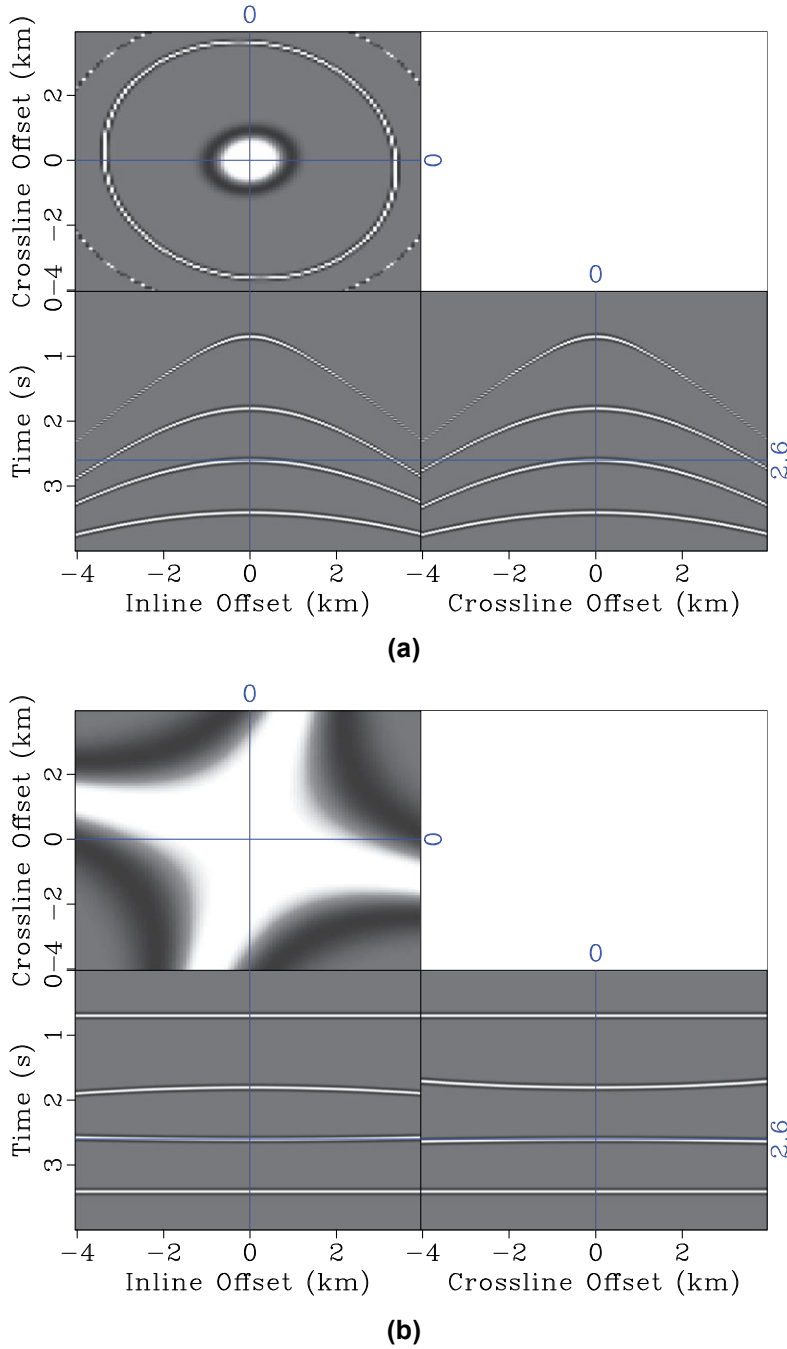


**Figure 2** 3D synthetic CMP gather (a) before and (b) after isotropic NMO.  $N_t = 1000$ ;  $N_x = N_y = 100$ .  $\Delta t = 0.004$  second;  $\Delta x = \Delta y = 80$  m.

all possible  $\mathbf{x}$  and  $\mathbf{k}$  (so it is mainly determined by the range of variables  $(f, x, y)$  and  $(\tau, p, q)$ ). A crucial property of this structure is that, at arbitrary level  $l$ , the side lengths  $w(A)$  of a box  $A$  in  $T_X$  and  $w(B)$  of a box  $B$  in  $T_K$  always satisfy  $w(A)w(B) = 1/N$ . Then when  $\mathbf{x}$ ,  $\mathbf{k}$  restricted in  $A$  and  $B$ , respectively, one can construct a low-rank (i.e., the number of terms in the expansion is small) separated expansion

for the kernel function  $\exp(2\pi i\Phi(\mathbf{x}, \mathbf{k}))$  (via a 3D Chebyshev interpolation):

$$\left| \exp(2\pi i\Phi(\mathbf{x}, \mathbf{k})) - \sum_{r=1}^{r_\epsilon} \alpha_r^{AB}(\mathbf{x}) \beta_r^{AB}(\mathbf{k}) \right| < \epsilon, \quad (12)$$

where  $\epsilon$  is a small constant controlling the error, and  $r_\epsilon$  is the

**Figure 3** Semblance plot (event 3) computed by the fast algorithm.  $N_t = 1000$ ;  $N_{W_{\cos}} = N_{W_{\sin}} = 100$ .

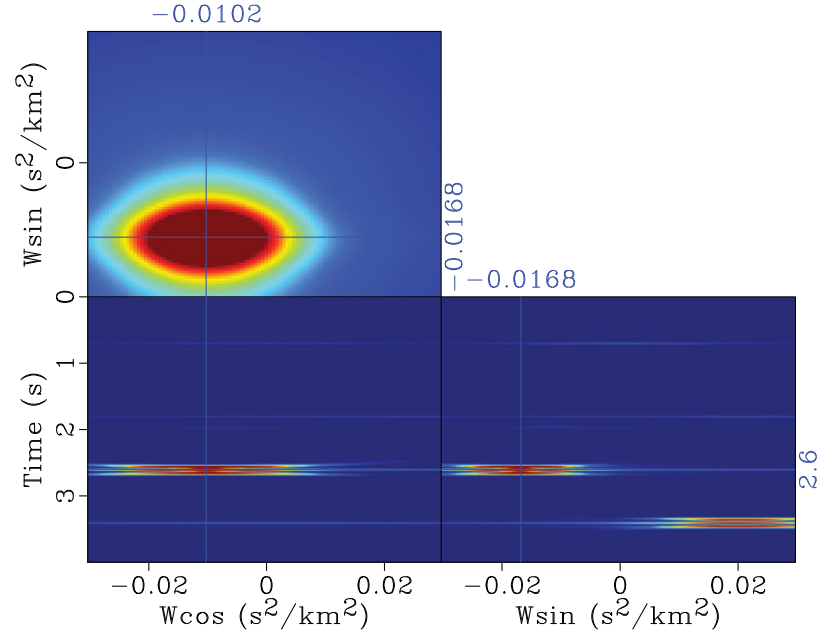
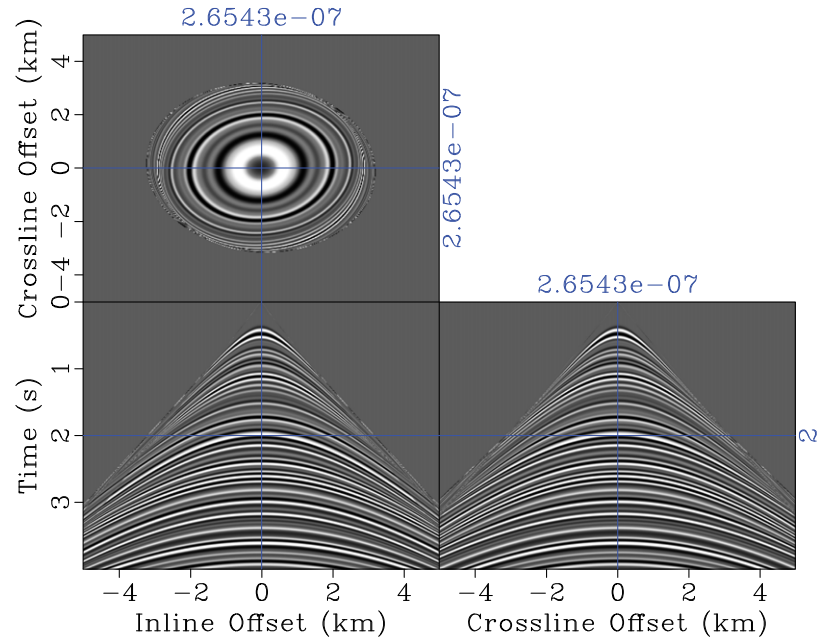


**Figure 4** 3D synthetic CMP gather.  $N_t = 1000$ ;  $N_x = N_y = 400$ .  $\Delta t = 0.004$  second;  $\Delta x = \Delta y = 25$  m.



number of expansion. Hence, for  $\mathbf{x} \in A$  and  $\mathbf{k} \in B$ , we have

$$\begin{aligned}
 (Rg)(\mathbf{x}) &= \sum_{\mathbf{k}} \exp(2\pi i \Phi(\mathbf{x}, \mathbf{k})) \hat{g}(\mathbf{k}) \\
 &\approx \sum_{\mathbf{k}} \sum_r \alpha_r^{AB}(\mathbf{x}) \beta_r^{AB}(\mathbf{k}) \hat{g}(\mathbf{k}) \\
 &= \sum_r \alpha_r^{AB}(\mathbf{x}) \left( \sum_{\mathbf{k}} \beta_r^{AB}(\mathbf{k}) \hat{g}(\mathbf{k}) \right) \\
 &:= \sum_r \alpha_r^{AB}(\mathbf{x}) \delta_r^{AB}.
 \end{aligned} \tag{13}$$

The essence of the algorithm is as follows: the summation (10) for  $\mathbf{x}, \mathbf{k}$  belonging to the whole computational domains

$X$  and  $K$  is highly oscillatory (the degree of oscillations in the kernel  $\exp(2\pi i \Phi(\mathbf{x}, \mathbf{k}))$  is roughly determined by  $N$  as introduced above). However, when we restrict to subdomains  $A$  and  $B$  that satisfy a certain condition, i.e., at least one of them is small, the kernel is less or non-oscillatory, thus low rank. Then, locally, the summation over  $\mathbf{k}$  can be reduced to a small number of terms indexed by  $r$ . The quantity  $\delta_r^{AB}$  in equation (13) is the so-called *equivalent sources* following

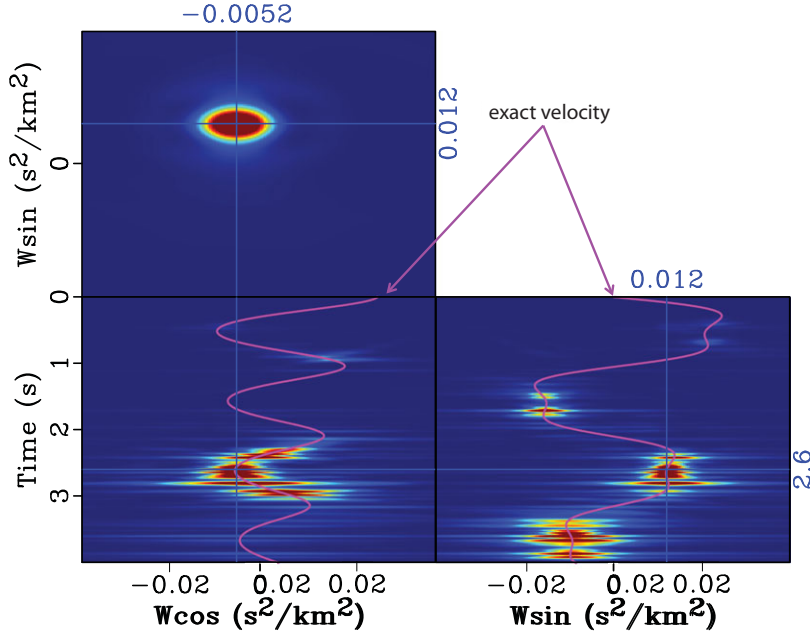


**Figure 5** Semblance plot computed by the fast algorithm.  $N_t = 1000$ ;  $N_{W_{\cos}} = N_{W_{\sin}} = 200$ . Purple curves overlaid are the exact  $W_{\cos}(\tau)$  and  $W_{\sin}(\tau)$ .

**Table 2** CPU time of direct velocity scan and fast butterfly algorithm for different  $N_{W_{\cos}}$  and  $N_{W_{\sin}}$  applied to the synthetic data in Fig. 4.

$N_{W_{\cos}} \times N_{W_{\sin}}$	direct velocity scan	fast butterfly algorithm	speedup factor
$10 \times 10$	1847 s	145 s	12.7
$20 \times 20$	7394 s	146 s	50.6
$100 \times 100$	$\sim 184700$ s	159 s	$\sim 1162$
$200 \times 200$	$\sim 738800$ s	196 s	$\sim 3769$

the nomenclature introduced by Candès, Demanet, and Ying (2009), i.e., instead of original sources  $g(k)$ , one deals with equivalent sources. In addition, if  $\delta_r^{AB}$  can be found for all boxes  $(A, B)$  with  $B = K$ , our problem will be solved. In order to do so, we need the butterfly structure. By embedding the low-rank expansion into the tree structure and traversing  $T_X$  from top to bottom and  $T_K$  from bottom to top, we arrive at a fast algorithm of only cubic complexity  $O(N^3 \log N)$  (there are  $N^3$  pairs of boxes  $(A, B)$  at every level, and there are  $\log N$  levels in total). Detailed description of the algorithm can be found in (Hu *et al.* 2013) where the difference between 2D and 3D formulations should be clear from the context.

Considering the initial Fourier transform for preparing data in the  $(f, x, y)$  domain, the overall complexity of our algorithm is roughly  $O(N_x N_y N_t \log N_t) + O(c(r_\epsilon)(N_f N_x N_y + N_t N_p N_q)) + O(C(r_\epsilon)N^3 \log N)$  ( $r_\epsilon$  terms are due to low-rank approximations, and the constant  $C(r_\epsilon)$  is bigger than  $c(r_\epsilon)$ ;

see (Hu *et al.* 2013) for more details). By comparison, the conventional straightforward velocity scan requires at least  $O(N_t N_p N_q N_x N_y)$  computations, which may quickly become a bottleneck as the problem size increases. Yet the efficiency of our algorithm is controlled mainly by  $O(N^3 \log N)$  with an  $\epsilon$ -dependent constant, where  $N$ , loosely put, depends on the maximum frequency and offset in the data set and the range of parameters in the model space. In practice,  $N$  can often be chosen smaller than the grid size.

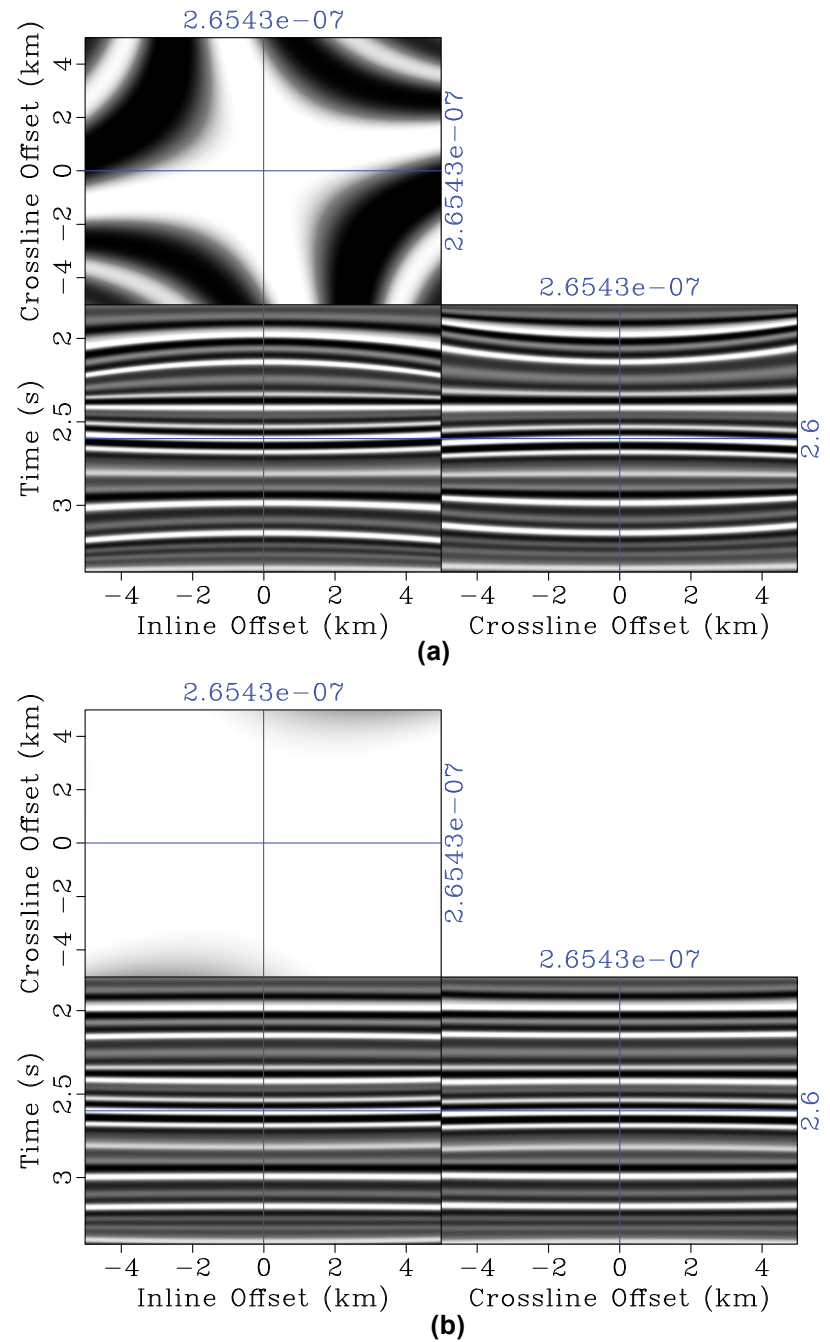
The significance the above analysis for the fast algorithm lies in the fact that the input and output data sizes  $N_t N_x N_y$  and  $N_t N_p N_q$  have little impact on the final computational cost; a dense sampling therefore becomes affordable.

## NUMERICAL EXAMPLES

In this section, we present several numerical examples to illustrate the empirical properties of the proposed fast algorithm. The emphasis will be put in comparing its performance with the straightforward velocity scan. Therefore, we deliberately neglect the choice of parameters in the algorithm to avoid too much detail<sup>3</sup>. In practice, there is no general rule to select  $N$  and the number of Chebyshev points used for low-rank approximation. They are usually set by trial and error. For instance, if the frequency bandwidth of the data is large, then

<sup>3</sup> All the examples will be made reproducible in Madagascar software package (Fomel *et al.* 2013).

**Figure 6** Synthetic gather (a) before and (b) after residual moveout using picked velocities from the semblance scan.



one may need more Chebyshev points in that direction. More discussions about the parameter choice are provided by Hu *et al.* (2013). To get a general idea, in the following examples, i.e.,  $N = 16$  or  $32$ , the number of Chebyshev points in each dimension of data or model domain is taken as 5, 7, or 9.

#### Example 1

We first consider a simple 3D synthetic CMP gather consisting of four isolated events, each with a different degree of azimuthal anisotropy (Fig. 2(a)). The moveout parameters  $\tau$ ,

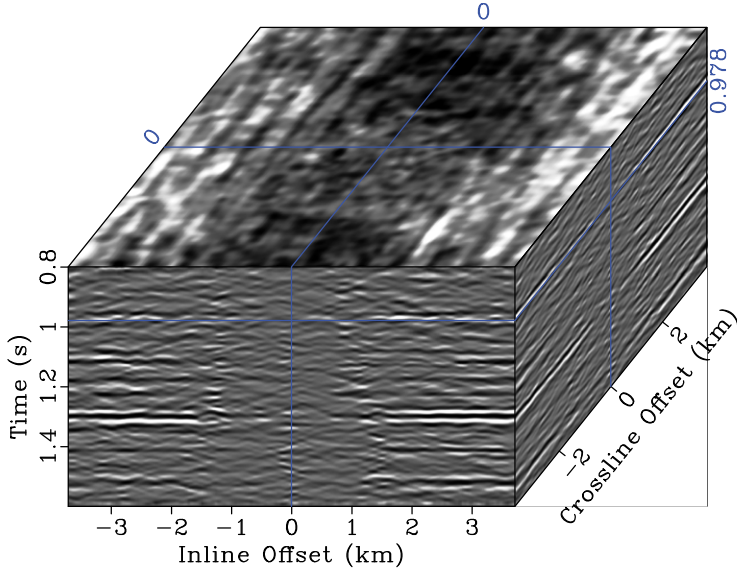


Figure 7 An isotropically NMO-corrected supergather from the McElroy data set, West Texas.  $N_t = 400$ ;  $N_x = N_y = 297$ .  $\Delta t = 0.002$  second;  $\Delta x = \Delta y = 25$  m.

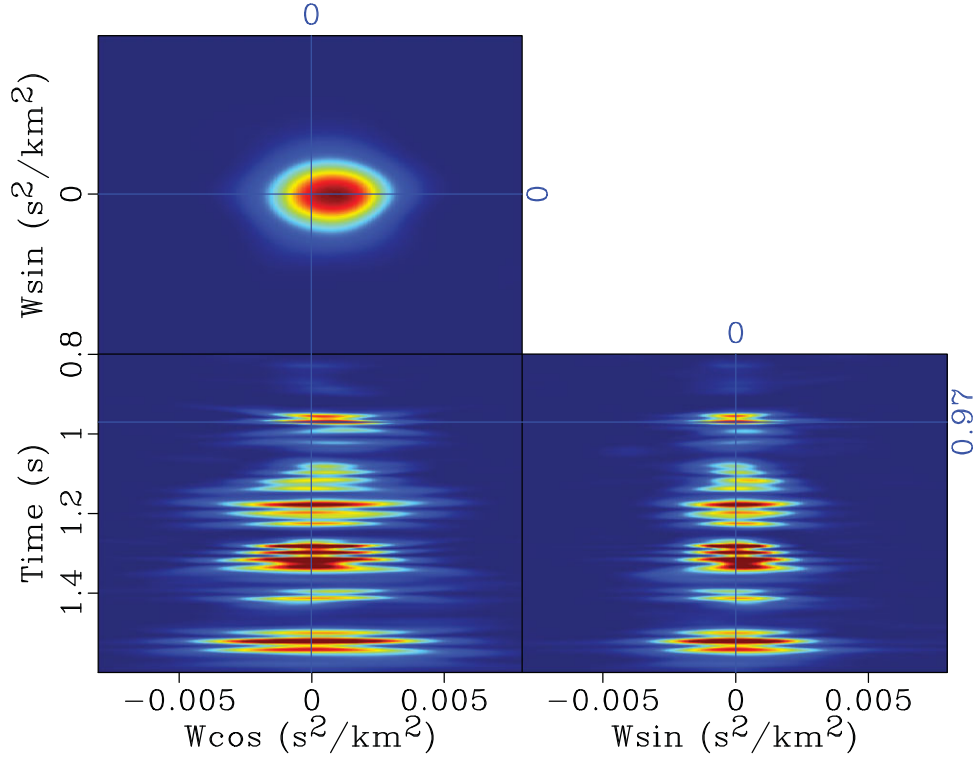


Figure 8 Semblance plot computed by the fast algorithm.  $N_t = 400$ ;  $N_{W_{\cos}} = N_{W_{\sin}} = 200$ .

$W_{\text{avg}}$ ,  $W_{\text{cos}}$ , and  $W_{\text{sin}}$  used to generate the events are specified in Table 1. Figure 2(b) shows the data after isotropic NMO using the exact  $W_{\text{avg}}$ . Except for the first flattened isotropic event, the other three events clearly require an additional moveout.

The computed semblance by the fast algorithm is shown in Fig. 3, where manually picked parameters coincide well with exact values. In addition to accuracy, what is remarkable is that, even for this moderate-sized problem ( $N_t = N_r = 1000$ ,

$N_x = N_y = N_{w_{\cos}} = N_{w_{\sin}} = 100$ ), the CPU time<sup>4</sup> of the butterfly algorithm (for a single stack) is about 139 second whereas the direct velocity scan takes 4681 second.

### Example 2

We now further investigate the properties of the fast algorithm using a more realistic 3D synthetic CMP gather (Fig. 4). The semblance plot computed by the fast algorithm is shown in Fig. 5. Figure 6(a) is the isotropically NMO-corrected data. After residual moveout using picked velocities from the semblance, curved events are flattened to the right position (Fig. 6(b)). We used an automatic picking algorithm from Fomel (2009) and Tao *et al.* (2012).

We next fix  $N_t = N_{\tau} = 1000$ ,  $N_x = N_y = 400$  and compare CPU time of the fast algorithm and the direct velocity scan for different  $N_{w_{\cos}}$  and  $N_{w_{\sin}}$  (Table 2). When  $N_{w_{\cos}}$  and  $N_{w_{\sin}}$  increase by a factor of 2, computation time of the direct velocity scan increases nearly by a factor of 4, which is consistent with our previous discussion on numerical complexity. On the other hand, CPU time of the fast algorithm is not affected much by the size of output sampling, again confirming our expectations.

### Example 3

Finally we consider a field data example. A subset of the McElroy data set from West Texas was formed in a supergather (Fig. 7). This data set was studied by Burnett and Fomel (2009a), in which they proposed a velocity-independent moveout correction to avoid costly velocity scan. With the fast algorithm, we are now able to compute the semblance efficiently: only 45 second for a single Radon transform when  $N_t = N_{\tau} = 400$ ,  $N_x = N_y = 297$ , and  $N_{w_{\cos}} = N_{w_{\sin}} = 200$ ; direct computation at this sampling would take approximately 30 hour.

Although the original data have been isotropically NMO corrected, the time slice still shows a subtle directional trend to flatness (Fig. 7). From the semblance plot (Fig. 8), we can observe some nonzero values of anisotropic parameters.

## CONCLUSIONS

We have introduced a fast approximate algorithm for azimuthally anisotropic 3D velocity scan. Compared with  $O(N^5)$

of the straightforward computation, our algorithm runs in  $O(N^3 \log N)$  time with a constant prefactor depending on the desired accuracy. The synthetic and field data experiments show that the method can be orders of magnitude faster than the conventional velocity scan, especially for large seismic data sets and dense parameter sampling. This, as a result, provides great potential to obtain better resolution for velocity picking.

To illustrate the proposed approach, we used a particular residual moveout function throughout the paper. The applicability of the butterfly algorithm is not limited to this form as long as the transform can be written in an oscillatory integral as demonstrated in the theory part. Possible additional applications include converted wave analysis and multifocusing analysis or common reflection surface.

## ACKNOWLEDGEMENTS

The authors would like to thank the associate editor and two anonymous reviewers for their valuable comments and suggestions, Chevron for the field data, and King Abdullah University of Science and Technology and sponsors of the Texas Consortium for Computational Seismology (TCCS) for financial support.

## REFERENCES

- Adler F. and Brandwood S. 1999. Robust estimation of dense 3D stacking velocities from automated picking. 69th Annual International SEG Meeting, Expanded Abstracts, 1162–1165.
- Arnaud, J., Rappin D., Dunand J.-P. and Curinier V. 2004. High density picking for accurate velocity and anisotropy determination. 74th Annual International SEG Meeting, Expanded Abstracts, 1627–1629.
- Beylkin G. 1984. The inversion problem and applications of the generalized Radon transform. *Communications on Pure and Applied Mathematics* 37, 579–599.
- Burnett W. and Fomel S., 2009a. 3D velocity-independent elliptically anisotropic moveout correction. *Geophysics* 74, WB129–WB136.
- Burnett W. and Fomel S. 2009b. Moveout analysis by time-warping. 79th Annual International Meeting, SEG, Expanded Abstracts, 3710–3714.
- Candès, E., Demanet L. and Ying L. 2009. A fast butterfly algorithm for the computation of Fourier integral operators. *Multiscale Modeling and Simulation* 7, 1727–1750.
- Casasanta L. 2011. NMO-ellipse independent 3D moveout analysis in  $\tau - p$  domain. 81st Annual International SEG Meeting, Expanded Abstracts, 289–294.
- Davidson M., Swan H., Sil S., Howell J., Olson R. and Zhou C. 2011. A robust workflow for detecting azimuthal anisotropy. 81st Annual International SEG Meeting, Expanded Abstracts, 259–263.
- Fomel S. 2009. Velocity analysis using AB semblance. *Geophysical Prospecting* 57, 311–321.

<sup>4</sup> Single-core performance on an Apple Macintosh equipped with 2.2-GHz Intel Core i7. Same for other examples.

- Fomel S., Sava P., Vlad I., Liu Y. and Bashkardin V., 2013. Madagascar: open-source software project for multidimensional data analysis and reproducible computational experiments. *Journal of Open Research Software* 1, e8.
- Fowler P. J., Jackson A. and Hootman B. 2006. Orthogonal parameters for anisotropic velocity analysis. 76th Annual International SEG Meeting, Expanded Abstracts, 169–173.
- Grechka V. and Tsvankin I., 1998. 3-D description of normal moveout in anisotropic inhomogeneous media. *Geophysics* 63, 1079–1092.
- Hu J., Fomel S., Demanet L. and Ying L. 2012. A fast butterfly algorithm for the hyperbolic Radon transform. 82nd Annual International SEG Meeting, Expanded Abstracts, 1–5.
- Hu J., Fomel S., Demanet L. and Ying L., 2013. A fast butterfly algorithm for generalized Radon transforms. *Geophysics* 78, U41–U51.
- Siliqi R., Meur D. L., Gamar F., Smith L., Toure J. P. and Herrmann P. 2003. High-density moveout parameter fields V and Eta. Part I: simultaneous automatic picking. 73rd Annual International SEG Meeting, Expanded Abstracts, 2088–2091.
- Taner M.T. and Koehler F., 1969. Velocity spectra-Digital computer derivation and applications of velocity functions. *Geophysics* 34, 859–881.
- Tao Y., Davidson M., Swan H., Fomel S., Malloy J., Howell J. *et al.* 2012. Constrained simultaneous automatic picking for VVAZ analysis. 82nd Annual International Meeting, SEG, Expanded Abstracts, 1–5.
- Tsvankin I. and Grechka V. 2011. Seismology of azimuthally anisotropic media and seismic fracture characterization. Society of Exploration Geophysicists.